CERN

Inference of Electromagnetic Boundary Data from Magnetic Measurements in Accelerator Magnets

Application to induction coil and Hall probe measurements

Melvin Liebsch[1,2], Stephan Russenschuck[1], Stefan Kurz[2]
[1]CERN, [2]Centre for Computational Engineering, Darmstadt, Germany

Motivation

Field Harmonics

- Physical representation of integrated and homogeneous fields
- Implying Maxwells equations: $\mathrm{div}\boldsymbol{B} = 0$, $\mathrm{curl}\boldsymbol{H} = \boldsymbol{0}$.
- If field is known at some radius, multipole theory provides **scaling laws** to interpolate into the cross-section

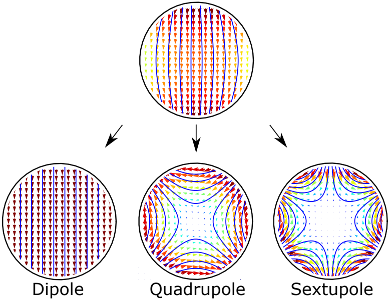

3D Field Representation by Boundary Data

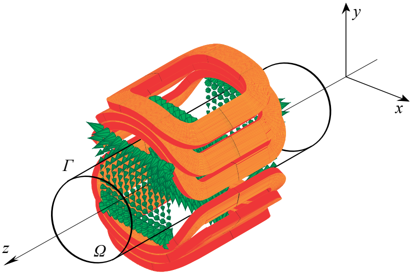

3D Field Representation by Boundary Data

Where we care about fringe fields:

- Spectrometers
- Detector magnets
- Large diameter focusing lenses [1]

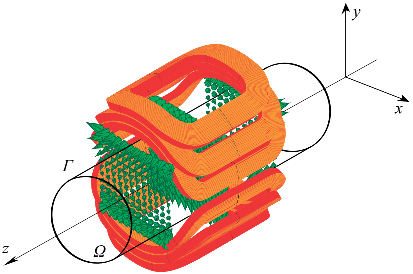

3D Field Representation by Boundary Data

Where we care about fringe fields:

- Spectrometers
- Detector magnets
- Large diameter focusing lenses [1]

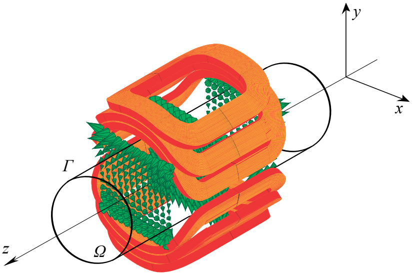

What is the benefit of a representation by boundary data:

- Reduces the amount of measurements needed to obtain a field map
- Smooths out spurious solutions.

Introduction

Local Field Measurement

Faraday's Law Transducers [2][3][4][5]

Rotating Coils

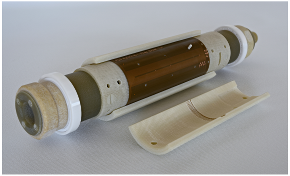

Translating Coils

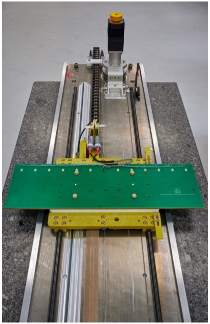

$U_{\text{ind}} = \int_{\partial \mathcal{A}} (\boldsymbol{v} \times \boldsymbol{B})\, \mathrm{d}\boldsymbol{r}$

+ Linear transfer function
+ Long time experience in calibration
+ High accuracy
- Large active areas

Hall Effect Sensors

+ Active area ~ 0.01 mm^2
+ 3 component measurement
- Nonlinear transfer function
- Temperature dependencies
- Elaborate calibration

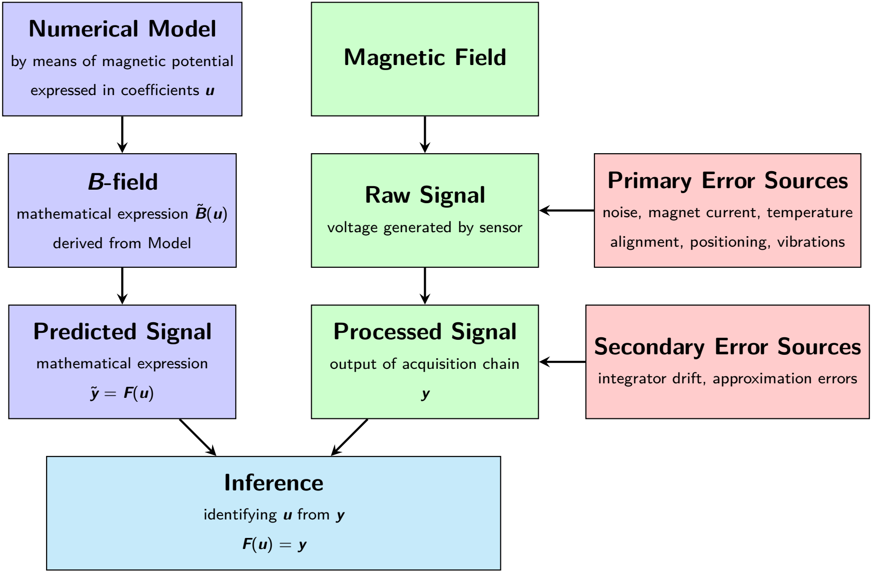
Numerical Model
by means of magnetic potential
expressed in coefficients $\boldsymbol{u}$
Magnetic Field
$\boldsymbol{B}$-field
mathematical expression $\tilde{\boldsymbol{B}}(\boldsymbol{u})$
derived from Model
Raw Signal
voltage generated by sensor
Primary Error Sources
noise, magnet current, temperature
alignment, positioning, vibrations
Predicted Signal
mathematical expression
$\tilde{\boldsymbol{y}} = \boldsymbol{F}(\boldsymbol{u})$
Processed Signal
output of acquisition chain
$\boldsymbol{y}$
Secondary Error Sources
integrator drift, approximation errors
Inference
identifying $\boldsymbol{u}$ from $\boldsymbol{y}$
$\boldsymbol{F}(\boldsymbol{u}) = \boldsymbol{y}$

Numerical Model

$$\boldsymbol{u} = (C_1, \dots, C_n)^T$$

$$A_z(r, \varphi) = \sum_n r^n C_n \exp(jn\varphi)$$

Magnetic Field

***B*-field**

$$\boldsymbol{B}(r, \varphi, \boldsymbol{u}) = \nabla \times \boldsymbol{A}$$

Raw Signal

$$U_{\text{ind}} = \int_\Gamma (\boldsymbol{v} \times \boldsymbol{B}) \mathrm{d}\boldsymbol{r}$$

Primary Error Sources

noise, magnet current, temperature

alignment, positioning, vibrations

Predicted Signal

$$\Phi(\varphi) = \int_{\mathcal{A}} \boldsymbol{B} \mathrm{d}\boldsymbol{a}$$

$$y_n = \mathcal{F}\{\Phi(\varphi)\} = s_n C_n$$

Processed Signal

$$\Delta\Phi_k \approx \int_{t_{k-1}}^{t_k} U_{\text{ind}} \mathrm{d}t$$

$$\Phi_k \approx \sum_{j=0}^{k} \Delta\Phi_k$$

$$y_n = \mathrm{DFT}(\Phi_k)$$

Secondary Error Sources

integrator drift, approximation errors

Inference

$$\begin{pmatrix} s_1 & \dots & 0 \\ \vdots & \ddots & \vdots \\ 0 & \dots & s_N \end{pmatrix} \begin{pmatrix} C_1 \\ \vdots \\ C_N \end{pmatrix} = \begin{pmatrix} y_1 \\ \vdots \\ y_N \end{pmatrix}$$

Numerical Model

$\boldsymbol{u} = (C_1, \ldots, C_n)^T$

$A_z(r, \varphi) = \sum_n r^n C_n \exp(jn\varphi)$

Magnetic Field

***B*-field**

$\boldsymbol{B}(r, \varphi, \boldsymbol{u}) = \nabla \times \boldsymbol{A}$

Raw Signal

$U_{\text{ind}} = \int_\Gamma (\boldsymbol{v} \times \boldsymbol{B}) \mathrm{d}\boldsymbol{r}$

Primary Error Sources

noise, magnet current, temperature

alignment, positioning, vibrations

Predicted Signal

$\Phi(\varphi) = \int_{\mathcal{A}} \boldsymbol{B} \mathrm{d}\boldsymbol{a}$

$\tilde{y}_n = \mathcal{F}\{\Phi(\varphi)\} = s_n C_n$

Processed Signal

$\Delta\Phi_k \approx \int_{t_{k-1}}^{t_k} U_{\text{ind}} \mathrm{d}t$

$\Phi_k \approx \sum_{j=0}^{k} \Delta\Phi_k$

$y_n = \mathrm{DFT}(\Phi_k)$

Secondary Error Sources

integrator drift, approximation errors

Inference

$$\begin{pmatrix} s_1 & \cdots & 0 \\ \vdots & \ddots & \vdots \\ 0 & \cdots & s_N \end{pmatrix} \begin{pmatrix} C_1 \\ \vdots \\ C_N \end{pmatrix} = \begin{pmatrix} y_1 \\ \vdots \\ y_N \end{pmatrix}$$

We **cannot always find** a diagonal forward operator $\boldsymbol{F}(\boldsymbol{u})$

Examples:

- large populated matrices
- nonlinear functions of $\boldsymbol{u}$

How do we infer?

- In some cases it might be difficult to find a solution for $\boldsymbol{u} = \boldsymbol{F}^{-1}(\boldsymbol{y})$
- Examples:
  - Nonlinear $\boldsymbol{F}(\boldsymbol{u})$
  - Ill conditioned $\boldsymbol{F}$
  - Large dimensional problems
- For this reason we make use of **Bayesian inference**.

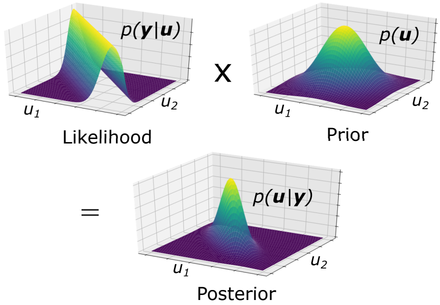

How do we infer?

- In some cases it might be difficult to find a solution for $\boldsymbol{u} = \boldsymbol{F}^{-1}(\boldsymbol{y})$
- Examples:
  - Nonlinear $\boldsymbol{F}(\boldsymbol{u})$
  - Ill conditioned $\boldsymbol{F}$
  - Large dimensional problems
- For this reason we make use of **Bayesian inference**.

Linear $\boldsymbol{F}$, Gaussian $p(\boldsymbol{y})$, $p(\boldsymbol{u})$:

$$p(\boldsymbol{u}|\boldsymbol{y}) \propto \exp\left(-\frac{1}{2}(\boldsymbol{u}-\boldsymbol{u}_1)^T \boldsymbol{Q}_1^{-1}(\boldsymbol{u}-\boldsymbol{u}_1)\right)$$

$$\boldsymbol{u}_1 = \boldsymbol{u}_0 + \boldsymbol{K}\underbrace{(\boldsymbol{y}-\boldsymbol{F}\boldsymbol{u}_0)}_{\text{Innovation}}$$

$$\boldsymbol{K} := \boldsymbol{Q}_0\boldsymbol{F}\left(\boldsymbol{F}\boldsymbol{Q}_0\boldsymbol{F}^T + \boldsymbol{R}\right)^{-1}$$

How do we infer?

- In some cases it might be difficult to find a solution for $\boldsymbol{u} = \boldsymbol{F}^{-1}(\boldsymbol{y})$
- Examples:
  - Nonlinear $\boldsymbol{F}(\boldsymbol{u})$
  - Ill conditioned $\boldsymbol{F}$
  - Large dimensional problems
- For this reason we make use of **Bayesian inference**.

Linear $\boldsymbol{F}$, Gaussian $p(\boldsymbol{y}), p(\boldsymbol{u})$:

$$p(\boldsymbol{u}|\boldsymbol{y}) \propto \exp\left(-\frac{1}{2}(\boldsymbol{u}-\boldsymbol{u}_1)^T \boldsymbol{Q}_1^{-1}(\boldsymbol{u}-\boldsymbol{u}_1)\right)$$

$$\boldsymbol{u}_1 = \boldsymbol{u}_0 + \boldsymbol{K}\underbrace{(\boldsymbol{y}-\boldsymbol{F}\boldsymbol{u}_0)}_{\text{Innovation}}$$

$$\boldsymbol{K} := \boldsymbol{Q}_0\boldsymbol{F}\left(\boldsymbol{F}\boldsymbol{Q}_0\boldsymbol{F}^T + \boldsymbol{R}\right)^{-1}$$

How to choose the prior?

- Prior Measurements
- Simulations
- ”Smoothing“ priors (zero mean) Tikhonov regularisation

Short Rotating Coil Measurement

Short Rotating Coil Scanners

Tangential

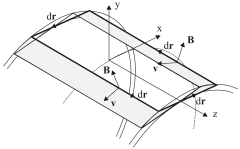

+ Multiple solid PCB
→ high accuracy track positioning

- Complicated $\boldsymbol{F}(\boldsymbol{u})$ due to B_ρ and B_z

Short Rotating Coil Scanners

Tangential

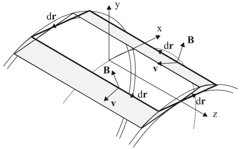

+ Multiple solid PCB
$\rightarrow$ high accuracy track positioning

- Complicated $\boldsymbol{F}(\boldsymbol{u})$ due to B_ρ and B_z

Iso-Perimetric [2]

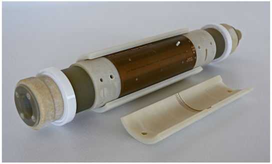

+ "Sees" B_ρ only
+ $\boldsymbol{F}$ = diagonal matrix

- Flexible PCB
$\rightarrow$ challenging track positioning

Short Rotating Coil Scanners

Tangential

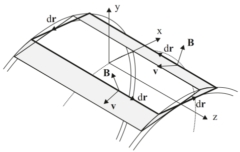

$+$ Multiple solid PCB
$\rightarrow$ high accuracy track positioning

- Complicated $\boldsymbol{F}(\boldsymbol{u})$ due to B_ρ and B_z

Iso-Perimetric [2]

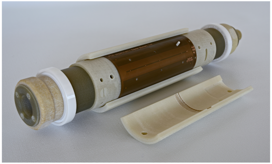

$+$ "Sees" B_ρ only
$+$ $\boldsymbol{F}$ = diagonal matrix

- Flexible PCB
$\rightarrow$ challenging track positioning

Radial

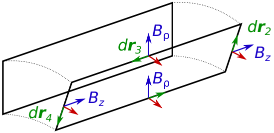

$+$ Whole coil array on a single, solid PCB
$\rightarrow$ high accuracy track positioning
$\rightarrow$ large bucking ratio

- Complicated $\boldsymbol{F}(\boldsymbol{u})$ due to B_ρ and B_z

Measurement Path

Magnetic Field → **Raw Signal** $U_{\text{ind}}(z_{\text{m}}) = \int_{\Gamma}(\boldsymbol{v} \times \boldsymbol{B})\mathrm{d}\boldsymbol{r}$ → **Processed Signal** $\boldsymbol{y}_n = (\Phi_n(z_1), ..., \Phi_n(z_M))^T$

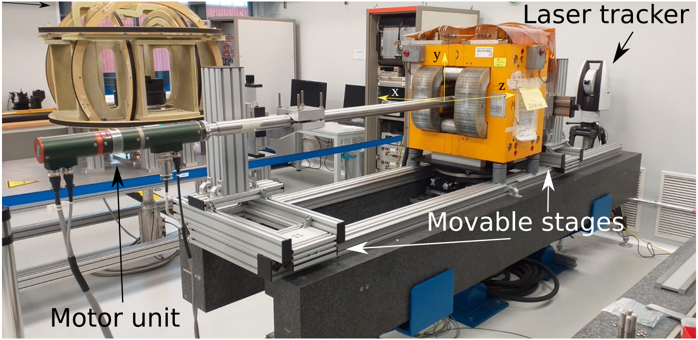

Test Example: Rotating Coil Sensor

Standard Radial Coil on PCB
Using a dipole bucking scheme

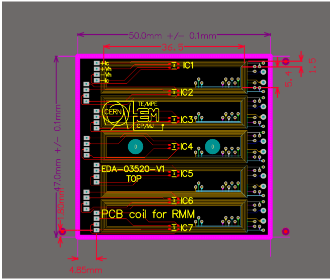

"Multipoles Extractor"

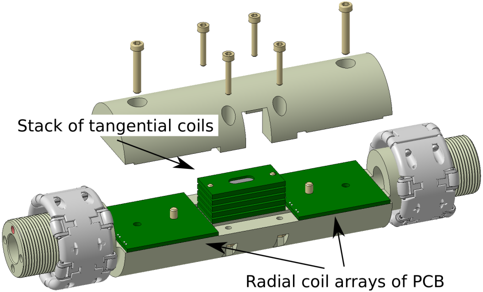

The Bessel-Fourier-Fourier Series

Numerical Model

$$\phi_{\mathrm{m}}(r,\varphi,z) = \frac{1}{2}\sum_{\substack{n=-\infty\\ n\neq 0}}^{\infty} \phi_n(r,z)\exp\left(jn\varphi\right)$$

$$\phi_n(r,z) = C_{0,n}r^{|n|} + \frac{1}{2}\sum_{\substack{k=-\infty\\ k\neq 0}}^{\infty} C_{k,n} I_{|n|}\left(\frac{2\pi|k|}{L}r\right)\exp\left(j\frac{2\pi k}{L}z\right)$$

Pros

+ Integrated field harmonics are encoded in $C_{0,n}$
+ "Maxwellian" solution even for truncated n, k-sum

Cons

- Bad scaling of $I_{|n|}(|k|r)$ for large n and k $\rightarrow$ **infeasible** for high k
- Expensive evaluation of Bessel functions $\rightarrow$ Pseudo-multipoles

Predicted Signal

$$\tilde{y}_n(z_m) = jn\mu_0 \left(C_{0,n} I_{1,n} + \frac{1}{2} \sum_{\substack{k=-K \\ k\neq 0}}^{K} C_{k,n} I_{2,n,k} I_{3,k} \right)$$

Geometric factors:

$$I_{1,n} = l \frac{(r_c + w/2)^{|n|} - (r_c - w/2)^{|n|}}{|n|},$$

$$I_{2,n,k} = \int_{r'=r_c-w/2}^{r_c+w/2} \frac{I_{|n|}\left(\frac{2\pi|k|}{L} r'\right)}{r'} \,\mathrm{d}r'$$

$$I_{3,k} = \frac{L}{\pi k} \sin\left(\frac{\pi k l}{L}\right) \exp\left(j \frac{2\pi k}{L} z_m\right).$$

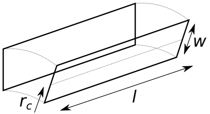

Numerical Model

$\phi_\mathrm{m}(r, \varphi, z)$

↓

***B*-field**

$\tilde{\boldsymbol{B}} = -\mu_0 \nabla \phi_\mathrm{m}$

↓

Predicted Signal

$\tilde{\Phi}(\varphi, z_m) = \int_{\mathcal{A}} \boldsymbol{B} \, \mathrm{d}\boldsymbol{a}$

$\tilde{y}_n(z_m) = \mathcal{F}\{\tilde{\Phi}(\varphi, z_m)\}$

$\tilde{\boldsymbol{y}} = (\tilde{\Phi}_n(z_1), \ldots, \tilde{\Phi}_n(z_M))^T$

Inference

- $\tilde{y}_n(z_m)$ is a linear function of $\boldsymbol{u} = (C_{-K,n}, \dots, C_{K,n})^T$
- We collect the geometric factors into a matrix $\boldsymbol{F}$ and obtain the equation system:

$$\boldsymbol{y}_n = \boldsymbol{F} \cdot \boldsymbol{u}$$

- We over-sample $M >> K$ and solve for $\boldsymbol{u}$ by least-squares.

Numerical Model

$\phi_{\mathrm{m}}(r, \varphi, z)$

↓

***B*-field**

$\tilde{\boldsymbol{B}} = -\mu_0 \nabla \phi_{\mathrm{m}}$

↓

Predicted Signal

$\Phi(\varphi, z_m) = \int_{\mathcal{A}} \boldsymbol{B} \, \mathrm{d}\boldsymbol{a}$

$\tilde{y}_n(z_m) = \mathcal{F}\{\Phi(\varphi, z_m)\}$

$\tilde{\boldsymbol{y}}_n = (\Phi_n(z_1), \dots, \Phi_n(z_M))^T$

Results

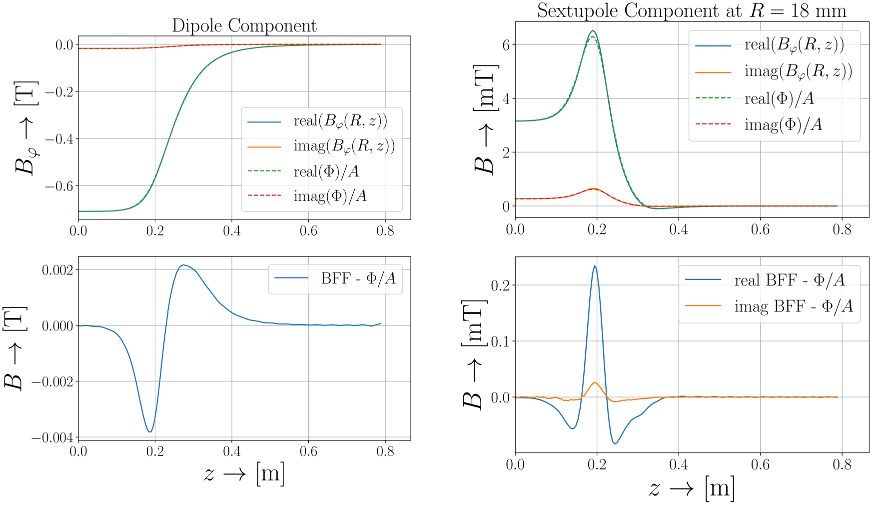

Dipole Component
$B_\varphi \to$ [T]
real($B_\varphi(R,z)$)
imag($B_\varphi(R,z)$)
real(Φ)/A
imag(Φ)/A
BFF - Φ/A
$B \to$ [T]
$z \to$ [m]
Sextupole Component at $R = 18$ mm
$B \to$ [mT]
real BFF - Φ/A
imag BFF - Φ/A

Scaling Laws

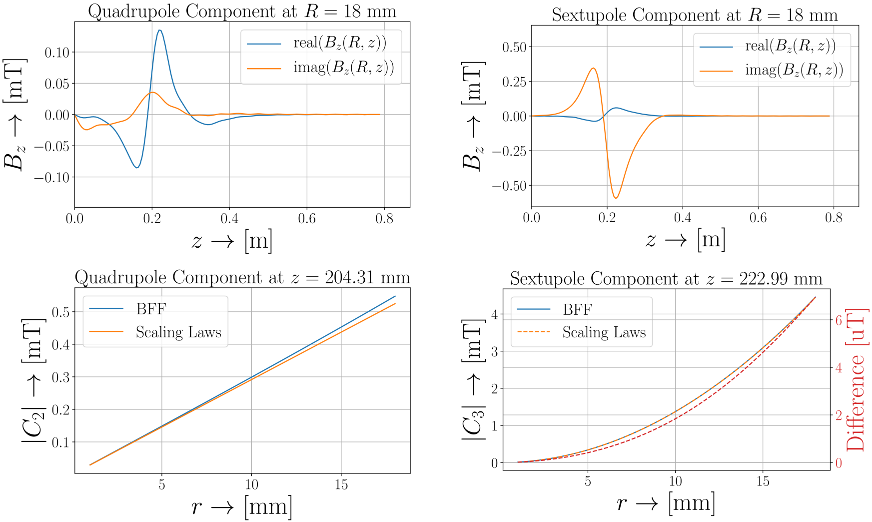

Summary

- Fringe field measurements with classical bucking schemes on solid PCB
  $\rightarrow$ increase resolution for higher multipole errors
  $\rightarrow$ cancellation of mechanical vibrations
- Approach can be applied to large diameter quadrupoles
- **We can avoid Hall probe measurements for local field measurement in cylindrical domains**

Translating Fluxmeter Measurement

Motivation

Large rectangular dipole magnets are often used in spectrometers.
The domain of interest Ω is box-shaped.

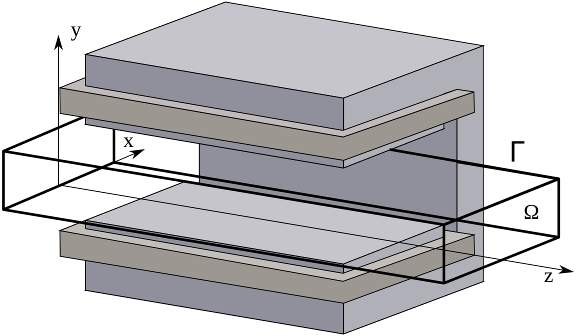

Motivation

The translating fluxmeter is specially designed for field homogeneity measurements in such magnets [5][6].

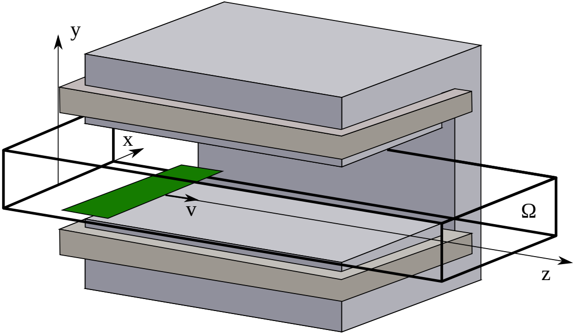

The Translating Fluxmeter

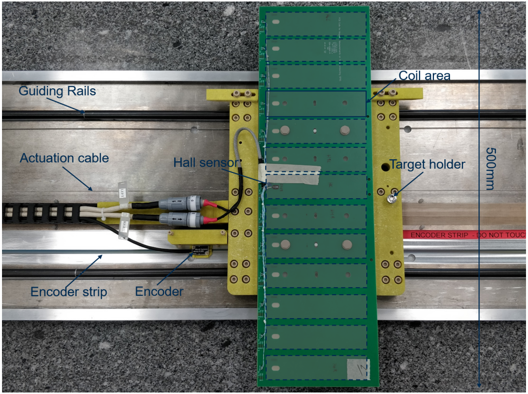

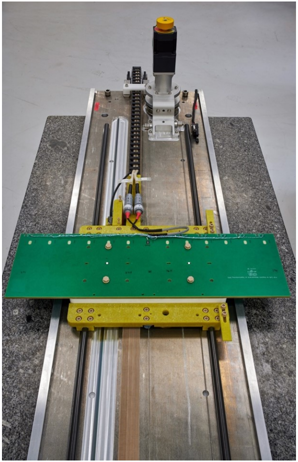

Maximum velocity of 0.6 m/s
Linear encoder with 5 um resolution
Compensated signals for homogeneity

Field Maps from Fluxmeter Measurements

Coils sampling on boundary

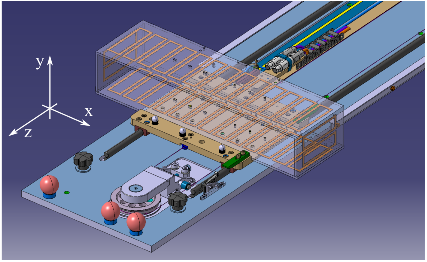

+ Direct measurement of boundary data
- Complicated sensor design
- Low field measurement for vertical coils

Sampling B_y inside the domain

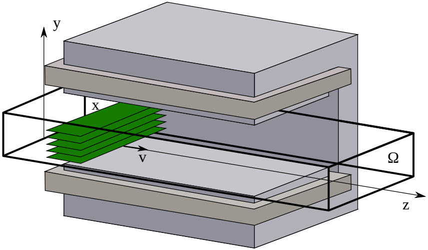

- Measurements are distributed throughout the domain
+ Vertical positioning can be adapted with spacers and dowel pins
+ Large signals for all coils

The Boundary Element Method

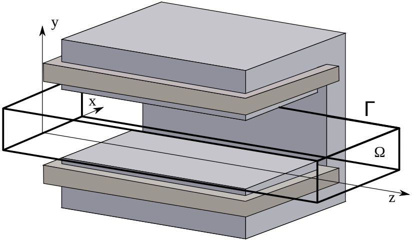

- The domain of interest is fully inscribed in the magnet bore.
- The magnet is too complex to derive an appropriate field model.

The Boundary Element Method

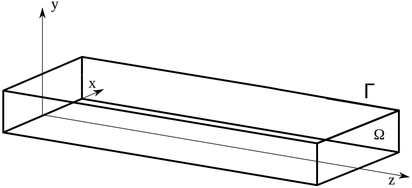

- The domain of interest is fully inscribed in the magnet bore.
- The magnet is too complex to derive an appropriate field model.
- We replace the magnet an express its effect in Ω by sheets of single and double layer potential on the domain boundary Γ.

Kirchhoff's integral equation

$$\phi_{\mathrm{m}}(\boldsymbol{r}) = \underbrace{\frac{1}{4\pi}\int_{\Gamma}\phi_{\mathrm{m}}(\mathrm{r}')\partial_{\mathbf{n}}\frac{1}{|\boldsymbol{r}-\boldsymbol{r}'|}\,\mathrm{d}\boldsymbol{r}'}_{\text{Double Layer Potential}} - \underbrace{\frac{1}{4\pi}\int_{\Gamma}\frac{1}{|\boldsymbol{r}-\boldsymbol{r}'|}\partial_{\mathbf{n}}\phi_{\mathrm{m}}(\mathrm{r}')\,\mathrm{d}\boldsymbol{r}'}_{\text{Single Layer Potential}}\,.$$

The Boundary Element Method

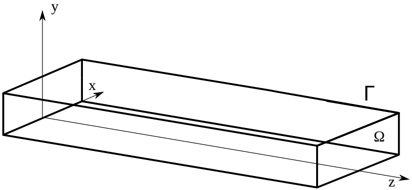

- The domain of interest is fully inscribed in the magnet bore.
- The magnet is too complex to derive an appropriate field model.
- We replace the magnet an express its effect in Ω by sheets of single and double layer potential on the domain boundary Γ.

Representation by Surface Currents [7]

$$\boldsymbol{A}(\boldsymbol{r}) = \frac{1}{4\pi} \int_{\Gamma} \frac{\mathrm{curl}_{\Gamma}\,\nu(\boldsymbol{r}')}{|\boldsymbol{r} - \boldsymbol{r}'|} \mathrm{d}\boldsymbol{r}'$$

Measurement Path

Magnetic Field

↓

Raw Signal

$$U_{\text{ind}} = \int_\Gamma (\boldsymbol{v} \times \boldsymbol{B})\mathrm{d}\boldsymbol{r}$$

↓

Processed Signal

$$\Delta\Phi_j \approx \int_{t_{j-1}}^{t_j} U_{\text{ind}}\mathrm{d}t$$

$$\Phi(z_k) \approx \sum_{j=0}^{k} \Delta\Phi_j$$

$$\boldsymbol{y} = (\Phi(z_1), \ldots, \Phi(z_M))$$

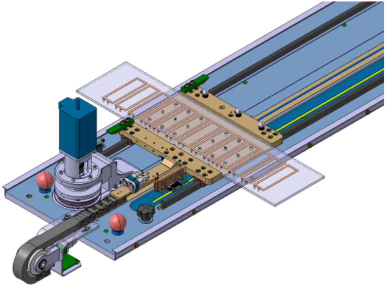

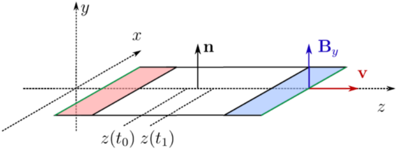

Predicted Signal

Numerical Model

$$\boldsymbol{A}(\boldsymbol{r}) = \frac{1}{4\pi} \sum_{n=1}^{N} u_n \int_\Gamma \frac{\mathrm{curl}_\Gamma \varphi(\boldsymbol{r}')}{|\boldsymbol{r}-\boldsymbol{r}'|} \mathrm{d}\boldsymbol{r}'$$

$\boldsymbol{B}$-field

$$\tilde{\boldsymbol{B}} = \mathrm{curl}\,\boldsymbol{A}$$

Predicted Signal

$$\tilde{y}(\boldsymbol{r}_m) = \int_{\mathcal{A}} \tilde{\boldsymbol{B}}\,\mathrm{d}\boldsymbol{a}$$
$$\tilde{y}(\boldsymbol{r}_m) = \int_{\Gamma} \boldsymbol{A}\,\mathrm{d}\boldsymbol{r}$$

$$\tilde{y}(\boldsymbol{r}_m) = \sum_{n=1}^{N} u_n \underbrace{\int_{\partial \mathcal{A}_m} \int_\Gamma \frac{\mathrm{curl}_\Gamma \varphi_n(\boldsymbol{r})}{4\pi|\boldsymbol{r}-\boldsymbol{r}'|} \mathrm{d}\boldsymbol{r}' \mathrm{d}\boldsymbol{r}}_{\text{geometric factors}}$$

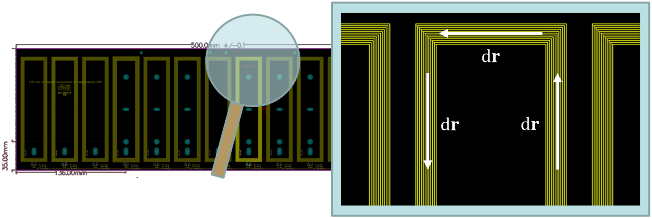

Inference

- We collect the geometric factors in a matrix $\boldsymbol{F}$:

$$\boldsymbol{y} = \boldsymbol{F} \cdot \boldsymbol{u}$$

- $\boldsymbol{F}$ is **ill conditioned**, due to the “blind eye” of the Sensor

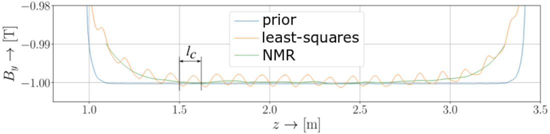

- We apply Bayesian inference for regularisation
- In this case (linear $\boldsymbol{F}$), Bayesian inference boils down to the Kálmán update:

$$\boldsymbol{u}_1 = \boldsymbol{u}_0 + \boldsymbol{K}(\boldsymbol{y} - \boldsymbol{F}\boldsymbol{u}_0)$$
$$\boldsymbol{K} := \boldsymbol{Q}_0 \boldsymbol{F} \left(\boldsymbol{F}\boldsymbol{Q}_0\boldsymbol{F}^T + \boldsymbol{R} \right)^{-1}$$

with an estimated noise covariance matrix $\boldsymbol{R}$ and Gaussian prior $\boldsymbol{u} \sim (\boldsymbol{u}, \boldsymbol{Q}_0)$.

Example: Measurements in Reference Dipole

- Fluxmeter is placed in C-shaped dipole
- Vertical position is modified by spacers between sledge and PCB
- Measurements at 5 vertical, and 13 horizontal positions $y \in (0\,,\,5\,,\,10\,,\,15\,,\,23)$ mm

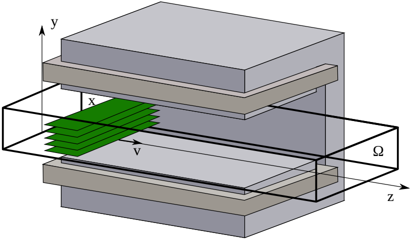

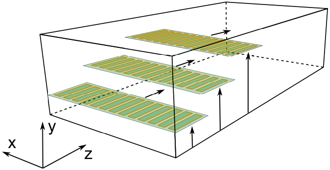

Example: Processed Data

- Measuremets in the center of the magnet

Flux measurements

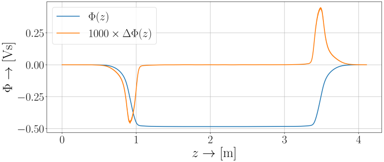

Standard deviation

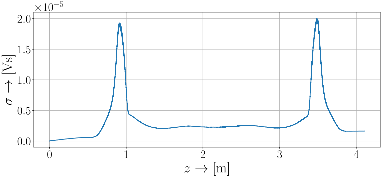

- Gaussian covariance matrix is estimated from 200 runs

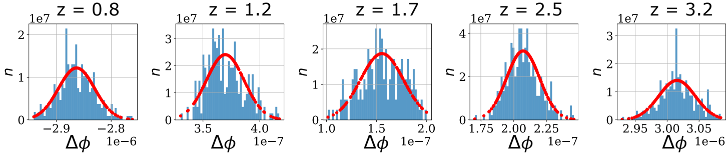

Example: Results

- Boundary data after Kálmán update:

Mean:

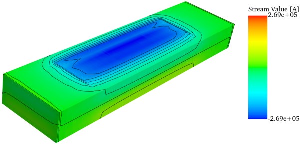

Variance:

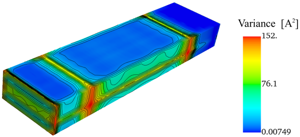

- Comparing field reconstruction with NMR in the homogeneous region

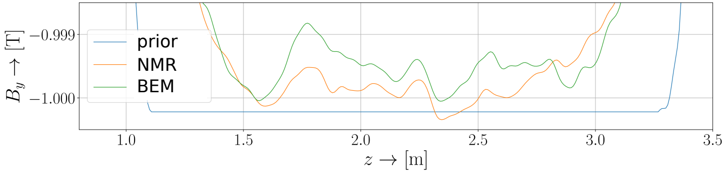

Reconstruction of Field Maps

At any position in Ω (here in the magnets center))

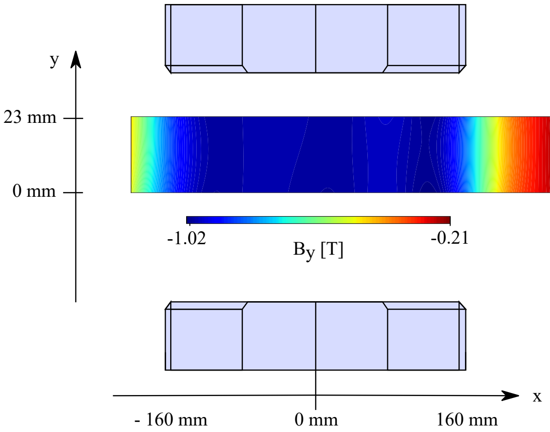

Summary

- We can use the translating fluxmeter to extract **field maps**
- **BEM** allows us to interpolate between the measurement positions
- **Bayesian inference** provides a regularisation of the ill-posed inference problem
- Coil layout can be optimised to improve sensitivity for higher frequency components

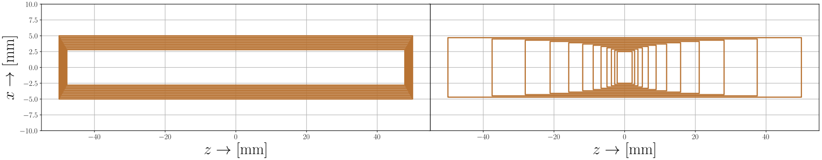

The Hall Probe Mapper System

The 3 axes Hall probe

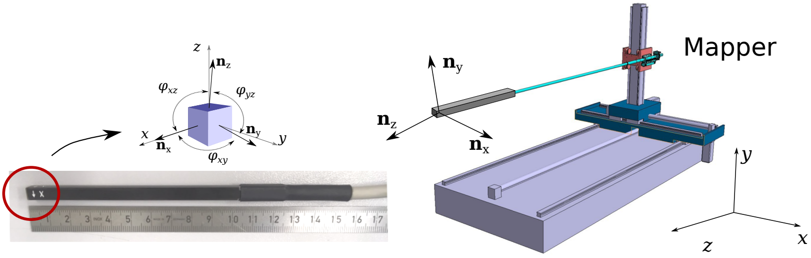

- Nonlinearities of individual axes are out calibrated in the measurement range at signal processing stage
- Three axes suffer from **large orientation errors** of ~ 2 deg
- The calibrated axis orientation is encoded by the unit vectors $\boldsymbol{n}_x$, $\boldsymbol{n}_y$ and $\boldsymbol{n}_z$ in our model

The FASER Permanent Dipole Magnets

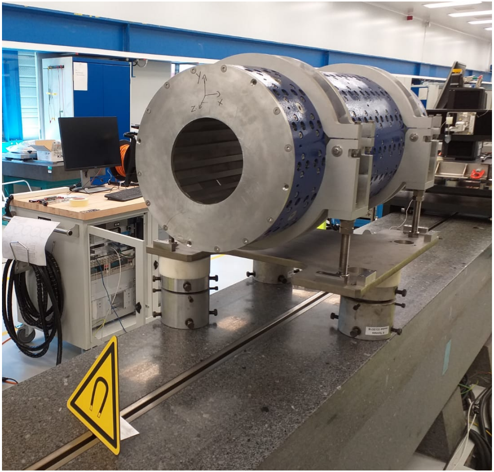

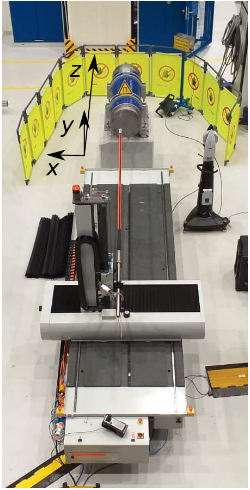

Measurement Procedure

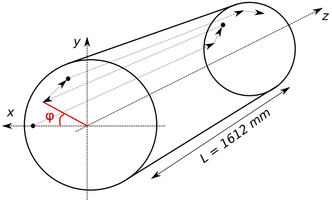

- We map along a cylindrical surface
- Moves are performed along *z*-axis
- Acquisition is done "one-the-fly" with 1 mm stepsize
- $\varphi = 3^\circ$ yielding 120 moves along z
- Total number of measurements $3 \times 120 \times 1612 = 583\,560$
- **The amount of data is too large to handle in a single inference step**

We infer the measurements "move-by-move", in successive Bayesian updates

Measurement Path (each move)

Raw Signal

$$U_x(\boldsymbol{r}_m) = s_x(\boldsymbol{B})$$
$$U_y(\boldsymbol{r}_m) = s_y(\boldsymbol{B})$$
$$U_z(\boldsymbol{r}_m) = s_z(\boldsymbol{B})$$

$\downarrow$

Processed Signal

$$U_x(\boldsymbol{r}_m) \approx s_x \boldsymbol{n}_x \cdot \boldsymbol{B}(\boldsymbol{r}_m) + U_{0,x}$$
$$U_y(\boldsymbol{r}_m) \approx s_y \boldsymbol{n}_y \cdot \boldsymbol{B}(\boldsymbol{r}_m) + U_{0,y}$$
$$U_z(\boldsymbol{r}_m) \approx s_z \boldsymbol{n}_z \cdot \boldsymbol{B}(\boldsymbol{r}_m) + U_{0,z}$$

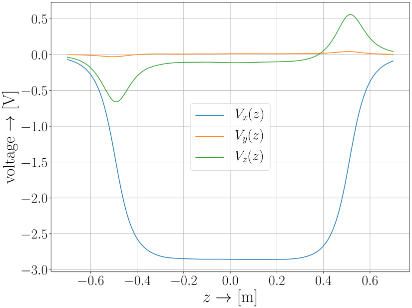

Predicted Signal (each move)

Numerical Model

$$\boldsymbol{A}(\boldsymbol{r}) = \frac{1}{4\pi}\sum_{n=1}^{N} u_n \int_\Gamma \frac{\mathrm{curl}_\Gamma \varphi(\boldsymbol{r}')}{|\boldsymbol{r}-\boldsymbol{r}'|}\mathrm{d}\boldsymbol{r}'$$

$\downarrow$

***B*-field**

$$\tilde{\boldsymbol{B}} = \mathrm{curl}\,\boldsymbol{A}$$

$\downarrow$

Predicted Signal

$$\tilde{U}_x(\boldsymbol{r}_m) = s_x\,\boldsymbol{n}_x \cdot \tilde{\boldsymbol{B}}(\boldsymbol{r}_m) + U_{0,x}$$
$$\tilde{U}_y(\boldsymbol{r}_m) = s_y\,\boldsymbol{n}_y \cdot \tilde{\boldsymbol{B}}(\boldsymbol{r}_m) + U_{0,y}$$
$$\tilde{U}_z(\boldsymbol{r}_m) = s_z\,\boldsymbol{n}_z \cdot \tilde{\boldsymbol{B}}(\boldsymbol{r}_m) + U_{0,z}$$

Predicted Signal (each move)

Numerical Model

$$\boldsymbol{A}(\boldsymbol{r}) = \frac{1}{4\pi} \sum_{n=1}^{N} u_n \int_\Gamma \frac{\mathrm{curl}_\Gamma \varphi(\boldsymbol{r}')}{|\boldsymbol{r}-\boldsymbol{r}'|} \mathrm{d}\boldsymbol{r}'$$

$\downarrow$

***B*-field**

$$\tilde{\boldsymbol{B}} = \mathrm{curl}\,\boldsymbol{A}$$

$\downarrow$

Predicted Signal

$$\tilde{U}_x(\boldsymbol{r}_m) = s_x\, \boldsymbol{n}_x \cdot \tilde{\boldsymbol{B}}(\boldsymbol{r}_m) + U_{0,x}$$
$$\tilde{U}_y(\boldsymbol{r}_m) = s_y\, \boldsymbol{n}_y \cdot \tilde{\boldsymbol{B}}(\boldsymbol{r}_m) + U_{0,y}$$
$$\tilde{U}_z(\boldsymbol{r}_m) = s_z\, \boldsymbol{n}_z \cdot \tilde{\boldsymbol{B}}(\boldsymbol{r}_m) + U_{0,z}$$

Inference

$\boldsymbol{F}_i$ encodes the geometric factors of $s_j\, \boldsymbol{n}_j \cdot \tilde{\boldsymbol{B}} + U_{0,j}$ for $j = x, y, z$

Prior $\boldsymbol{u}_0$, $\boldsymbol{Q}_0$

$\downarrow$

$\boldsymbol{u}_{i-1}$, $\boldsymbol{Q}_{i-1}$

$\downarrow$

Measure along z at φ_i

$\downarrow \boldsymbol{y}_i$

Kálmán update

$$\boldsymbol{u}_i = \boldsymbol{u}_{i-1} + \boldsymbol{K}_i\left(\boldsymbol{y}_i - \boldsymbol{F}_i \boldsymbol{u}_{i-1}\right)$$

$\boldsymbol{u}_i$ $\boldsymbol{Q}_i$

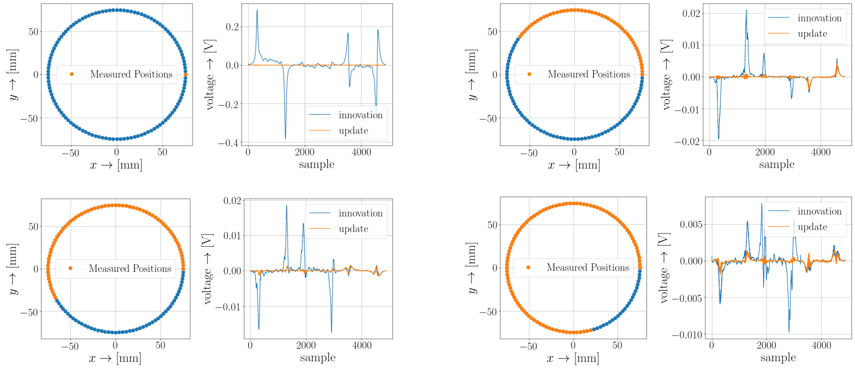

Measured Positions
$y \rightarrow$ [mm]
$x \rightarrow$ [mm]
innovation
update
voltage $\rightarrow$ [V]
sample
Measured Positions
$y \rightarrow$ [mm]
$x \rightarrow$ [mm]
innovation
update
voltage $\rightarrow$ [V]
sample
Measured Positions
$y \rightarrow$ [mm]
$x \rightarrow$ [mm]
innovation
update
voltage $\rightarrow$ [V]
sample
Measured Positions
$y \rightarrow$ [mm]
$x \rightarrow$ [mm]
innovation
update
voltage $\rightarrow$ [V]
sample

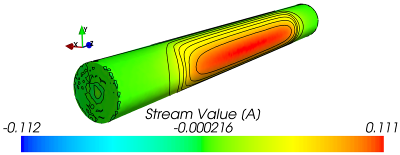
Stream Value (A)
-0.112
-0.000216
0.111

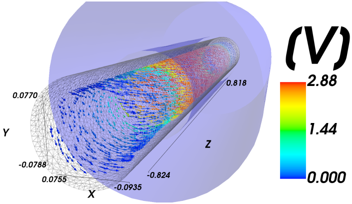
(V)
2.88
1.44
0.000
0.0770
0.818
Y
Z
-0.0788
0.0755
-0.824
-0.0935
X

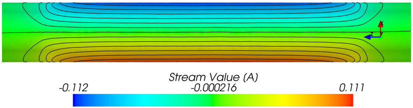
Stream Value (A)
-0.112
-0.000216
0.111

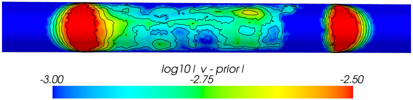
log10 | v - prior |
-3.00
-2.75
-2.50

Field Reconstruction

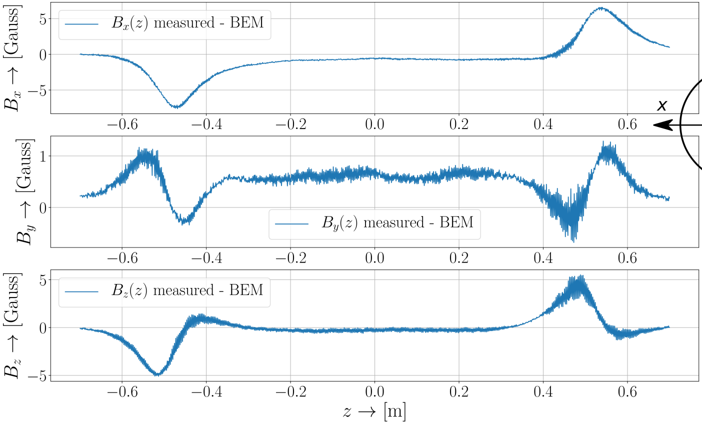

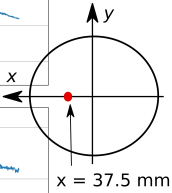

Summary

- Bayesian inference allows us to infer large amounts of data **iteratively**
- **Total measurement time is reduced** since only the boundary needs to be measured
- Bayesian updates are faster than measurements. Updates can be implemented **on the measurement bench**.
- **Noise is smoothed out** in the field reconstruction
- Bayesian inference comes with **uncertainty quantification** “for free”

Acknowledgements

The work of Melvin Liebsch is supported by the 'Excellence Initiative' of the German Federal and State Governments and the Graduate School of Computational Engineering at Technische Universität Darmstadt.

References

A. Simona, *Numerical methods for the simulationof particle motion in electromagneticfields.* Phd thesis, Politecnico Milano and Technische Universität Darmstadt, 2020.

G. Caiafa, P. Arpaia, and R. Stephan, "A rotating-coil magnetometer for scanning transversal field harmonics in accelerator magnets," *Scientific Reports*, vol. 9, 06 2019.

C. Daniele, "Design and development of a translating-coil magnetometer - master thesis," 2016.

A. Windischofer, "Development of a new translating induction coil magnetometer in pcb technology - master thesis," 2020.

G. Golluccio, M. Buzio, D. Caltabiano, G. Deferne, O. Dunkel, L. Fiscarelli, D. Giloteaux, C. Petrone, S. Russenschuck, and P. Schnizer, "Instruments and Methods for the Magnetic Measurement of the Super-FRS Magnets," in *7th International Particle Accelerator Conference*, p. TUPMB037, 2016.

S. Russenschuck, "Rotating- and translating-coil magnetometers for extracting pseudo-multipoles in accelerator magnets," *COMPEL - The international journal for computation and mathematics in electrical and electronic engineering*, vol. 36, pp. 00–00, 07 2017.

J. D. Jackson, *Classical electrodynamics; 2nd ed.* New York, NY: Wiley, 1975.

home.cern